Figures and figure supplements

LIPG signaling promotes tumor initiation and metastasis of human basal-like triple-negative breast cancer

Pang-Kuo Lo *et al*

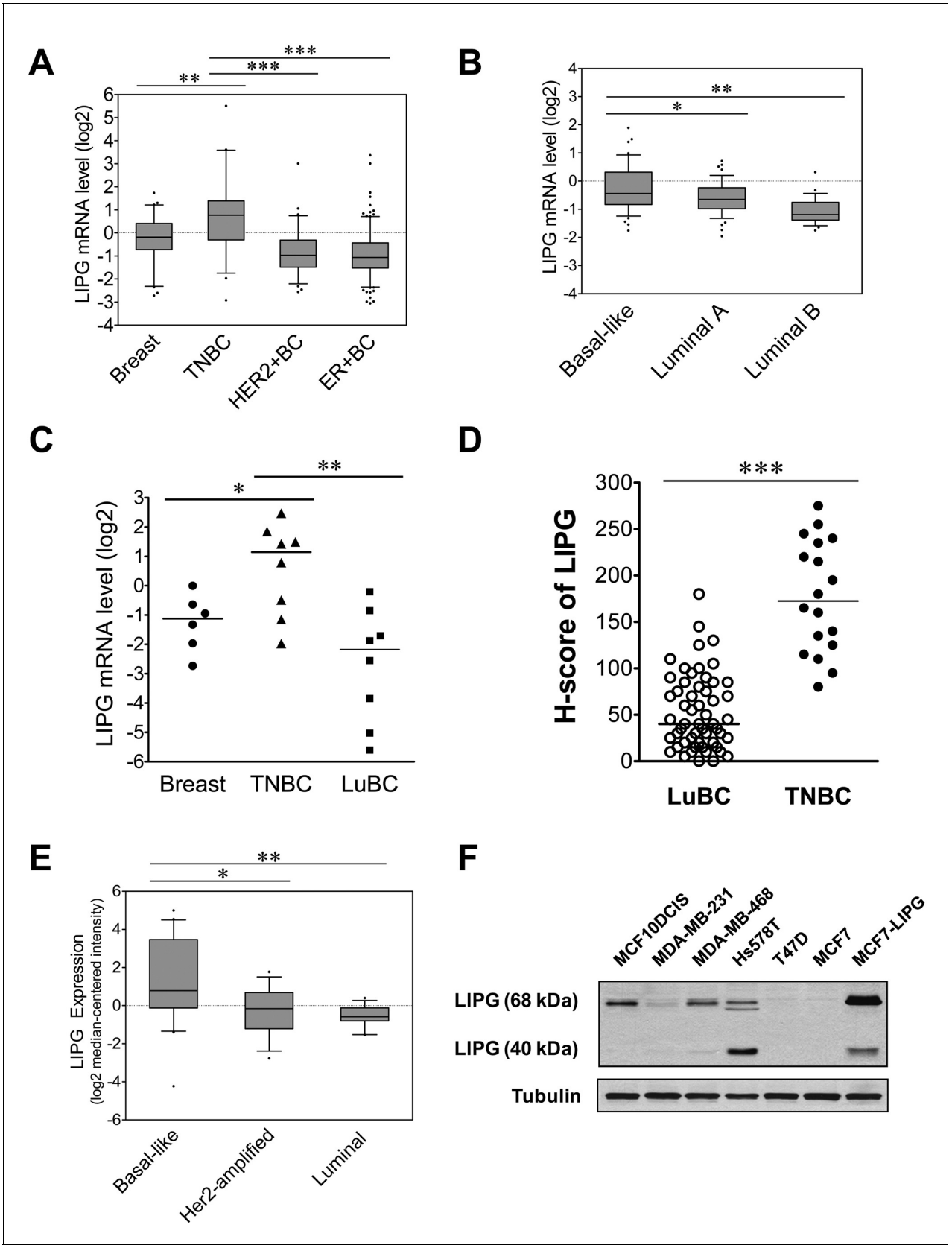

Figure 1. LIPG is aberrantly overexpressed in basal-like TNBC. (**A**) LIPG mRNA expression in normal breast and different subtypes of breast cancers based on *in silico* analysis of the TCGA dataset. Normal breast (n = 61), TNBC (n = 46), HER2+ BC (n = 67) and ER+ BC (n = 225). The 25th and 75th

Figure 1 continued on next page

Figure 1 continued

percentiles are indicated as a vertical box and the 5th and 95th percentiles are indicated as outliers. (**B**) LIPG mRNA expression in different molecular subtypes of breast cancer classified based on the PAM50 gene expression signature. Expression of LIPG mRNA in basal-like (n = 45), luminal-A (n = 46) and luminal-B (n = 25) breast cancers was analyzed *in silico* using the Gluck dataset collected in the Oncomine database. The 25th and 75th percentiles are indicated as a vertical box and the 10th and 90th percentiles are indicated as outliers. (**C**) qRT-PCR analysis of LIPG mRNA expression in normal breast, TNBC and ER+ PR+ HER2- luminal breast cancers (LuBC). (**D**) LIPG protein expression in TNBC and LuBC according to H-scoring of IHC-stained tissues using the anti-LIPG antibody. A total of 55 LuBC and 18 TNBC cases were analyzed in the IHC experiment. Horizontal lines indicate medians of IHC datasets. (**E**) LIPG mRNA expression in different molecular subtypes of breast cancer cell lines. Expression of LIPG mRNA in basal-like (n = 20), Her2-amplified (n = 15) and luminal (n = 13) breast cancer cell lines was analyzed *in silico* using the Hoeflich dataset retrieved from the Oncomine database. The 25th and 75th percentiles are indicated as a vertical box and the 10th and 90th percentiles are indicated as outliers. (**F**) LIPG protein expression in breast cancer cell lines. MCF7-LIPG is a LIPG-overexpresing MCF7 cell line. Tubulin was used as a loading control. *p<0.05; **p<0.01; ***p<0.001.

DOI: https://doi.org/10.7554/eLife.31334.002

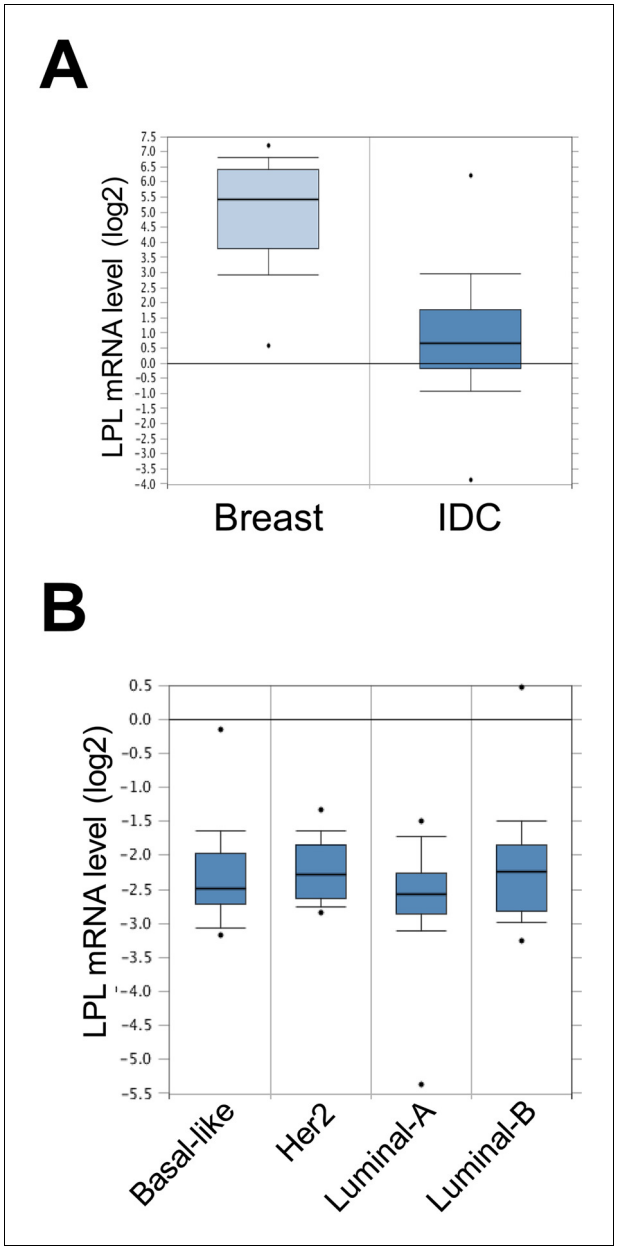

Figure 1—figure supplement 1. Expression of LPL is downregulated in breast cancer. (**A**) Expression of LPL mRNA in normal breast (n = 61) and invasive ductal carcinomas (IDC, n = 389). (**B**) Expression of LPL mRNA in basal-like (n = 45), Her2 (n = 21), luminal-A (n = 46) and luminal-B (n = 25) subtypes of breast cancer.
DOI: https://doi.org/10.7554/eLife.31334.003

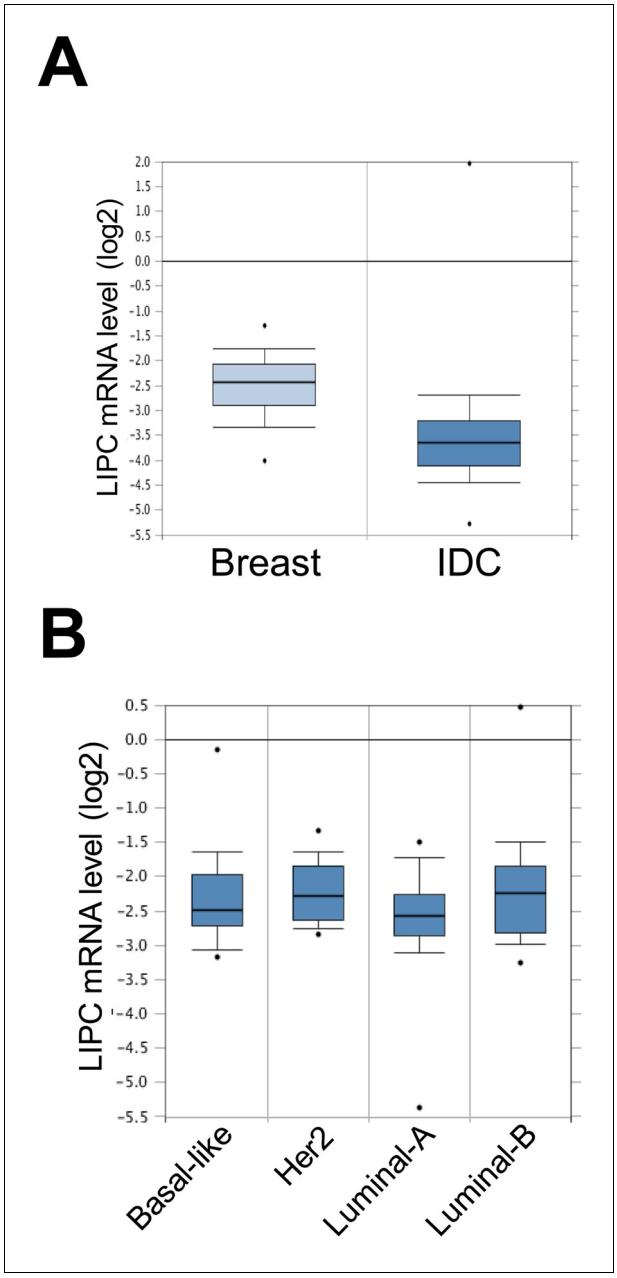

Figure 1—figure supplement 2. Expression of LIPC is downregulated in breast cancer. (**A**) Expression of LIPC mRNA in normal breast (n = 61) and invasive ductal carcinomas (IDC, n = 389). (**B**) Expression of LIPC mRNA in basal-like (n = 45), Her2 (n = 21), luminal-A (n = 46) and luminal-B (n = 25) subtypes of breast cancer.
DOI: https://doi.org/10.7554/eLife.31334.004

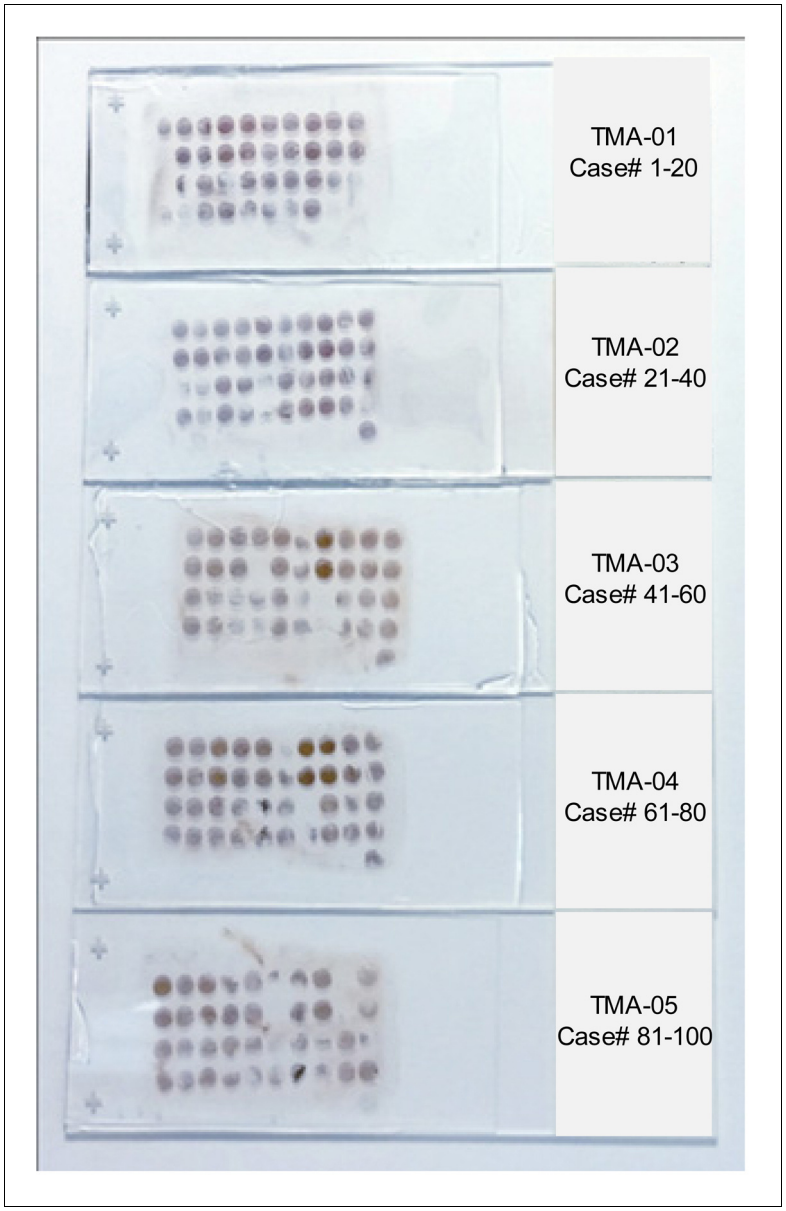

Figure 1—figure supplement 3. IHC analysis of LIPG protein expression was performed on tissue microarrays of breast cancer. Each tissue microarray slide contained 20 different breast cancer tissue specimens and a duplicate of each breast cancer tissue specimen was included. Five different tissue microarray slides that encompassed a total of 100 breast cancer tissue specimens were stained in the IHC experiment. A total of 66 cases of tissue duplicates were successfully stained by the anti-LIPG antibody, including 47 luminal breast cancer and 10 TNBC cases.

DOI: https://doi.org/10.7554/eLife.31334.005

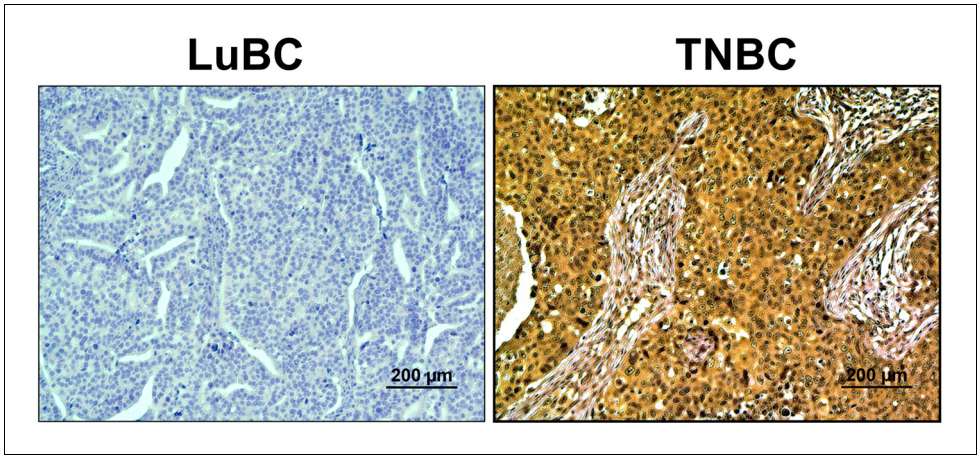

Figure 1—figure supplement 4. LIPG protein is overexpressed in TNBC. IHC analysis of LIPG protein expression in Luminal breast cancers (LuBC) and triple-negative breast cancers (TNBC).

DOI: https://doi.org/10.7554/eLife.31334.006

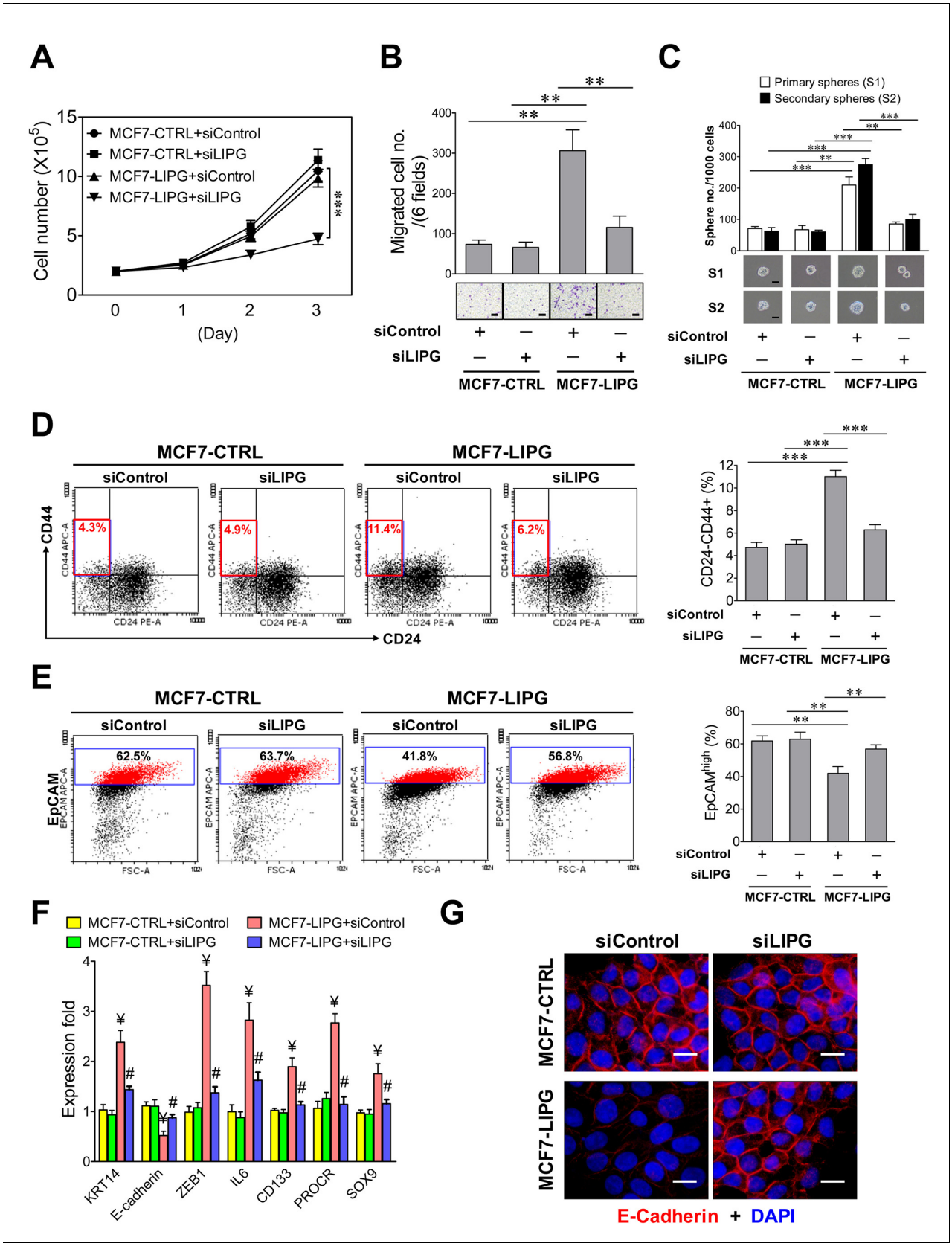

Figure 2. Ectopic overexpression of LIPG in LIPG-deficient luminal breast cancer cells promotes migration, stemness and basal/EMT features. (**A**) Growth of LIPG-overexpressing MCF7 cells, but not parental control cells, is inhibited by LIPG knockdown. 2 × 10^5 cells of MCF7-CTRL (the vector-

Figure 2 continued on next page

Figure 2 continued

control cells) and MCF7-LIPG (LIPG-overexpressing cells) transfected with either the control siRNA (siControl) or LIPG siRNA (siLIPG) were seeded for the 3-day cell growth study (n = 3 for each time point). (**B**) LIPG overexpression promotes migration of MCF7 cells. Triplicate transwell-based migration experiments were performed on siRNA-transfected cells as described in (**A**). The scale bar indicates 100 μm. (**C**) LIPG overexpression enhances the primary and secondary CSC sphere formation of MCF7. Triplicate primary sphere formation experiments were performed on siRNA-transfected cells as described in (**A**). After a week, primary spheres were counted and collected for siRNA transfections and secondary sphere formation analysis as described in 'Materials and methods'. The scale bar indicates 50 μm. (**D**) LIPG overexpression increases the CSC-enriched CD24-/CD44+ cell subset in MCF7 cells. Triplicate FACS analyses of the CD24/CD44 profile were performed on siRNA-transfected cells as described in (**A**). The representative FACS profiles of CD24/CD44 are shown on the left panel and the bar graph is shown on the right panel. (**E**) LIPG overexpression decreases the $EpCAM^{high}$ cell population in MCF7 cells. Triplicate FACS analyses of EpCAM vs. FSC (Forward Scatter parameter) were performed on siRNA-transfected cells as described in (**A**). The representative FACS profiles of EpCAM/FSC are shown on the left panel and the bar graph is shown on the right panel. (**F**) LIPG overexpression in MCF7 cells leads to the increased expression of basal/EMT and stem cell genes and downregulation of E-cadherin. qRT-PCR analysis of basal/EMT and stem cell genes was performed on siRNA-transfected cells as described in (**A**). ¥ $p<0.01$ versus the control datasets (MCF7-CTRL + siControl and MCF7-CTRL + siLIPG); # $p<0.05$ versus the dataset of MCF7-LIPG cells transfected with siControl (MCF7-LIPG + siControl); n = 3. (**G**) LIPG overexpression downregulates E-cadherin expression. Immunofluorescent analysis of E-cadherin protein expression was performed on siRNA-transfected cells as described in (**A**). Cellular DNA was stained with DAPI. The scale bar indicates 25 μm. Error, standard deviation (SD); **$p<0.01$; ***$p<0.001$.

DOI: https://doi.org/10.7554/eLife.31334.011

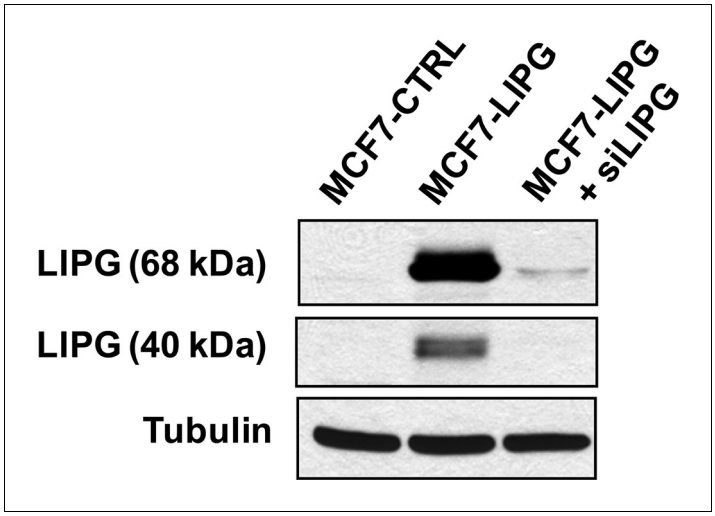

Figure 2—figure supplement 1. Western blot analysis of LIPG and tubulin protein expression in MCF7-CTRL, MCF7-LIPG and MCF7-LIPG plus LIPG knockdown.

DOI: https://doi.org/10.7554/eLife.31334.012

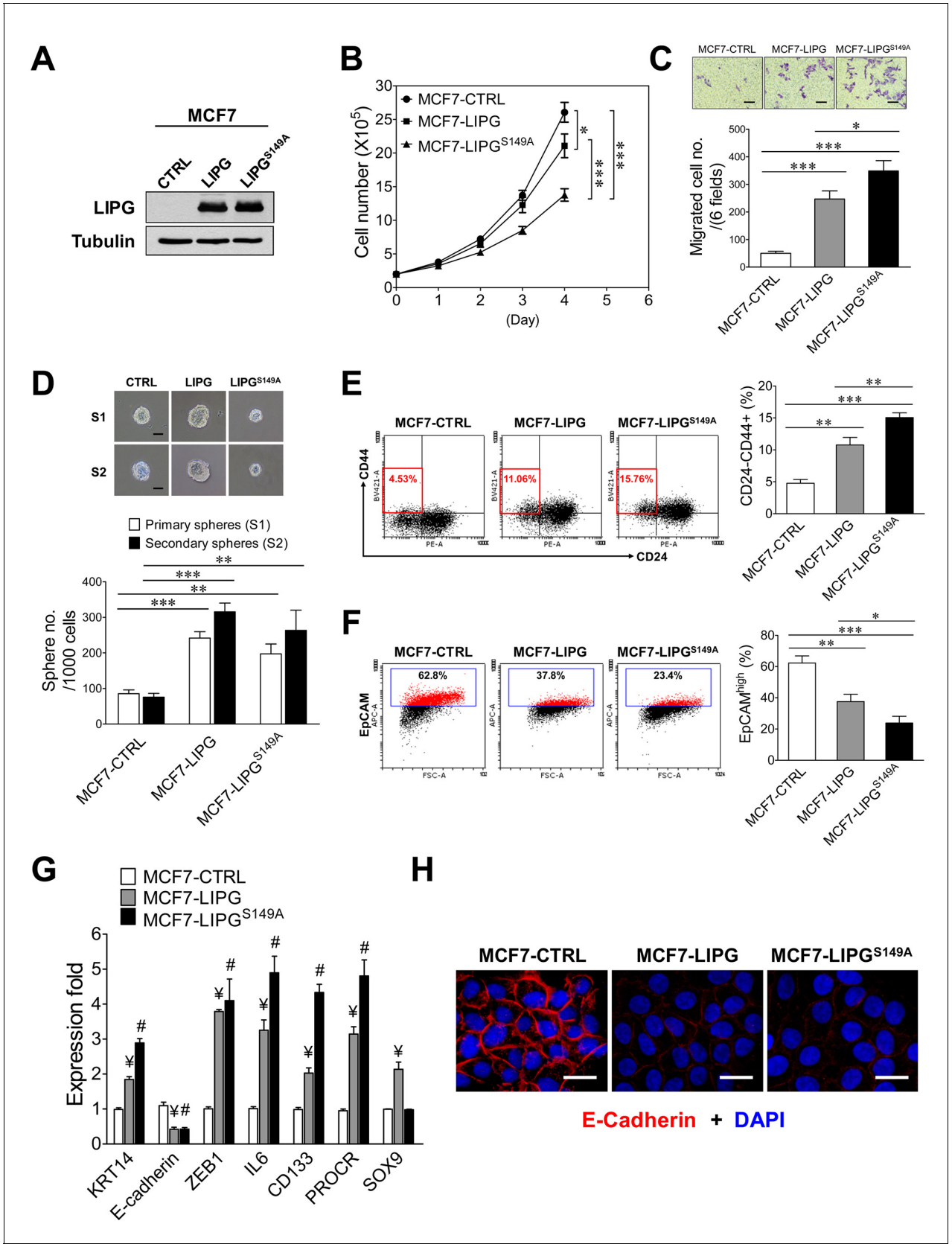

Figure 3. The lipase catalytic activity of LIPG is relevant to cell growth, but not to the motility, stemness and EMT of breast cancer cells. (**A**) Western blot analysis of LIPG and tubulin protein expression in vector-control (CTRL), wild-type LIPG-overexpressing (LIPG) and LIPG mutant-overexpressing

Figure 3 continued on next page

Figure 3 continued

(LIPG^{S149A}) MCF7 lines. (**B**) Loss of the lipase catalytic activity of LIPG attenuates cell growth. 2 × 10^5 cells of three MCF7 lines as described in (**A**) were seeded for the four-day cell growth study (n = 3 for each time point). (**C**) LIPG^{S149A} is potent to promote migration of MCF7 cells. Triplicate transwell-based migration experiments were performed on three MCF7 lines as described in (**A**). The scale bar indicates 100 μm. (**D**) LIPG^{S149A} is competent to enhance the primary and secondary CSC sphere formation of MCF7 but fails to promote sphere cell proliferation. Triplicate primary and secondary sphere formation experiments were performed on three MCF7 lines as described in (**A**). The scale bar indicates 50 μm. (**E**) LIPG^{S149A} overexpression increases the CSC-enriched CD24-/CD44+ cell subset in MCF7 cells. Triplicate FACS analyses of the CD24/CD44 profile were performed on three MCF7 lines as described in (**A**). The representative FACS profiles of CD24/CD44 are shown on the left panel and the bar graph is shown on the right panel. (**F**) LIPG^{S149A} overexpression decreases the EpCAM^{high} cell population in MCF7 cells. Triplicate FACS analyses of EpCAM vs. FSC were performed on three MCF7 lines as described in (**A**). The representative FACS profiles of EpCAM/FSC are shown on the left panel and the bar graph is shown on the right panel. (**G**) LIPG^{S149A} overexpression in MCF7 cells leads to the increased expression of basal/EMT and stem cell genes and downregulation of E-cadherin. qRT-PCR analysis of basal/EMT and stem cell genes was performed on three MCF7 lines as described in (**A**). ¥ $p<0.01$ versus the control dataset (MCF7-CTRL); # $p<0.01$ versus the control dataset (MCF7-CTRL); n = 3. (**H**) LIPG^{S149A} overexpression downregulates E-cadherin expression. Immunofluorescent analysis of E-cadherin protein expression was performed on three MCF7 lines as described in (**A**). Cellular DNA was stained with DAPI. The scale bar indicates 25 μm. Error, standard deviation (SD); *$p<0.05$; **$p<0.01$; ***$p<0.001$.

DOI: https://doi.org/10.7554/eLife.31334.014

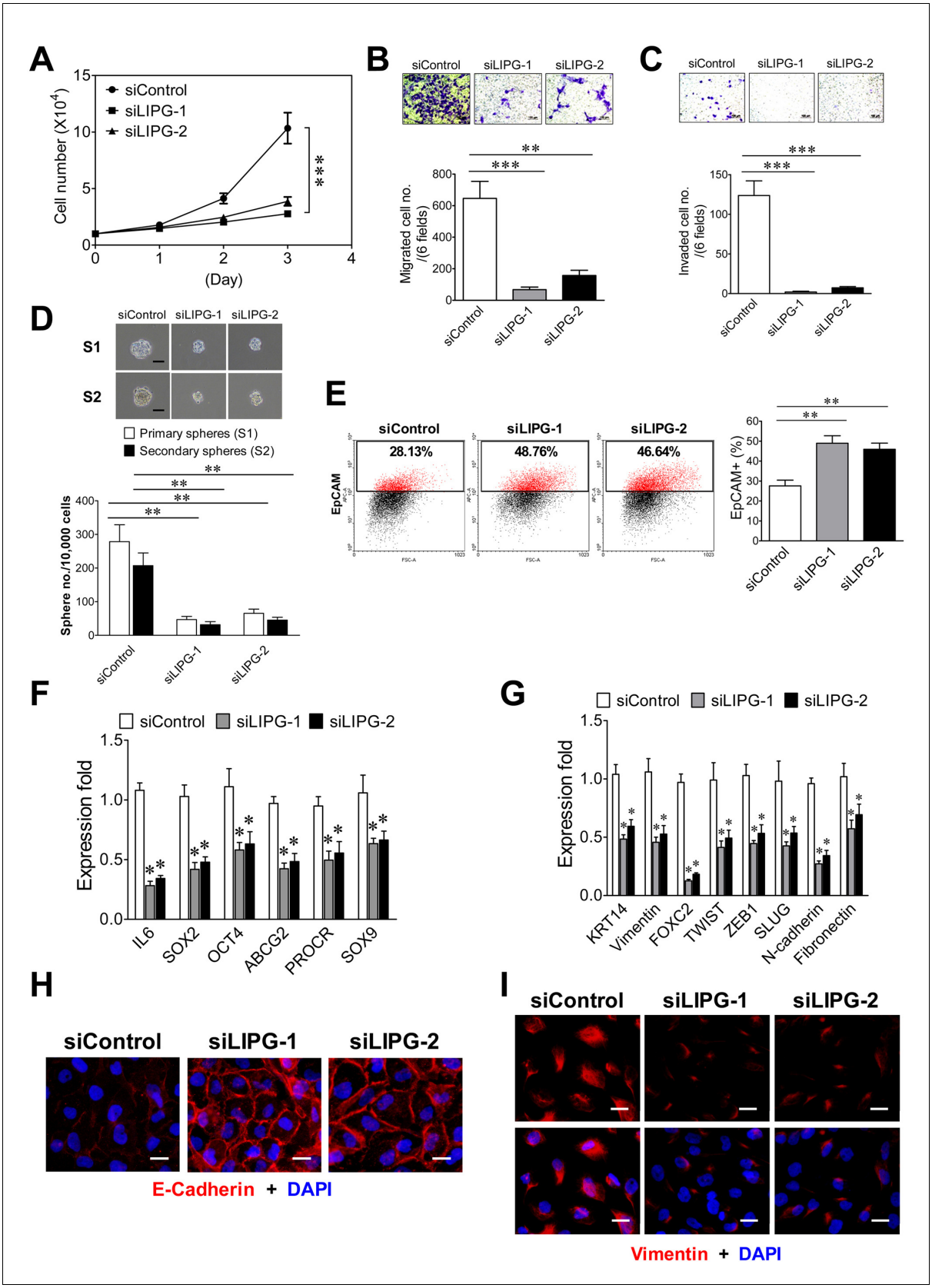

Figure 4. LIPG inactivation impairs invasiveness, stemness and basal/EMT features of basal-like DCIS cells. (**A**) LIPG knockdown inhibits cell growth of MCF10DCIS cells. 1 × 10^4 cells of siRNA-transfected cells were seeded for the three-day cell growth study. (**B**) LIPG knockdown impairs migration of

Figure 4 continued on next page

Figure 4 continued

MCF10DCIS cells. The scale bar indicates 100 μm. (**C**) LIPG knockdown suppresses invasion of MCF10DCIS cells. The scale bar indicates 100 μm. (**D**) LIPG knockdown leads to decreases in primary and secondary sphere formation of MCF10DCIS cells. The scale bar indicates 50 μm. (**E**) LIPG knockdown increases the EpCAM-positive cell population in MCF10DCIS cells. (**F**) LIPG knockdown results in the downregulation of stem cell gene expression in MCF10DCIS cells. (**G**) LIPG knockdown leads to the downregulation of basal/EMT gene expression. (**H**) LIPG knockdown causes increased E-cadherin expression in MCF10DCIS cells. Immunofluorescent analysis of E-cadherin was performed on siRNA-transfected MCF10DCIS cells. Cellular DNA was stained with DAPI. The scale bar indicates 25 μm. (**I**) LIPG knockdown gives rise to decreased vimentin expression in MCF10DCIS cells. Immunofluorescent analysis of vimentin was performed on siRNA-transfected MCF10DCIS cells. Cellular DNA was stained with DAPI. The scale bar indicates 25 μm. Error, SD (n = 3); *p<0.05; **p<0.01; ***p<0.001.

DOI: https://doi.org/10.7554/eLife.31334.016

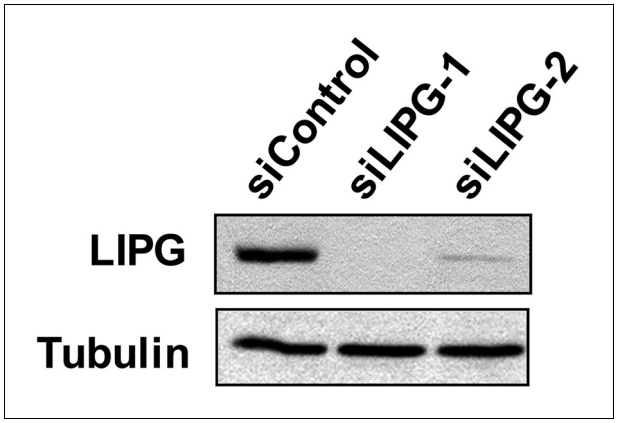

Figure 4—figure supplement 1. Western blot analysis of LIPG and tubulin protein expression in MCF10DCIS cells with or without LIPG knockdown by two different siRNAs.
DOI: https://doi.org/10.7554/eLife.31334.017

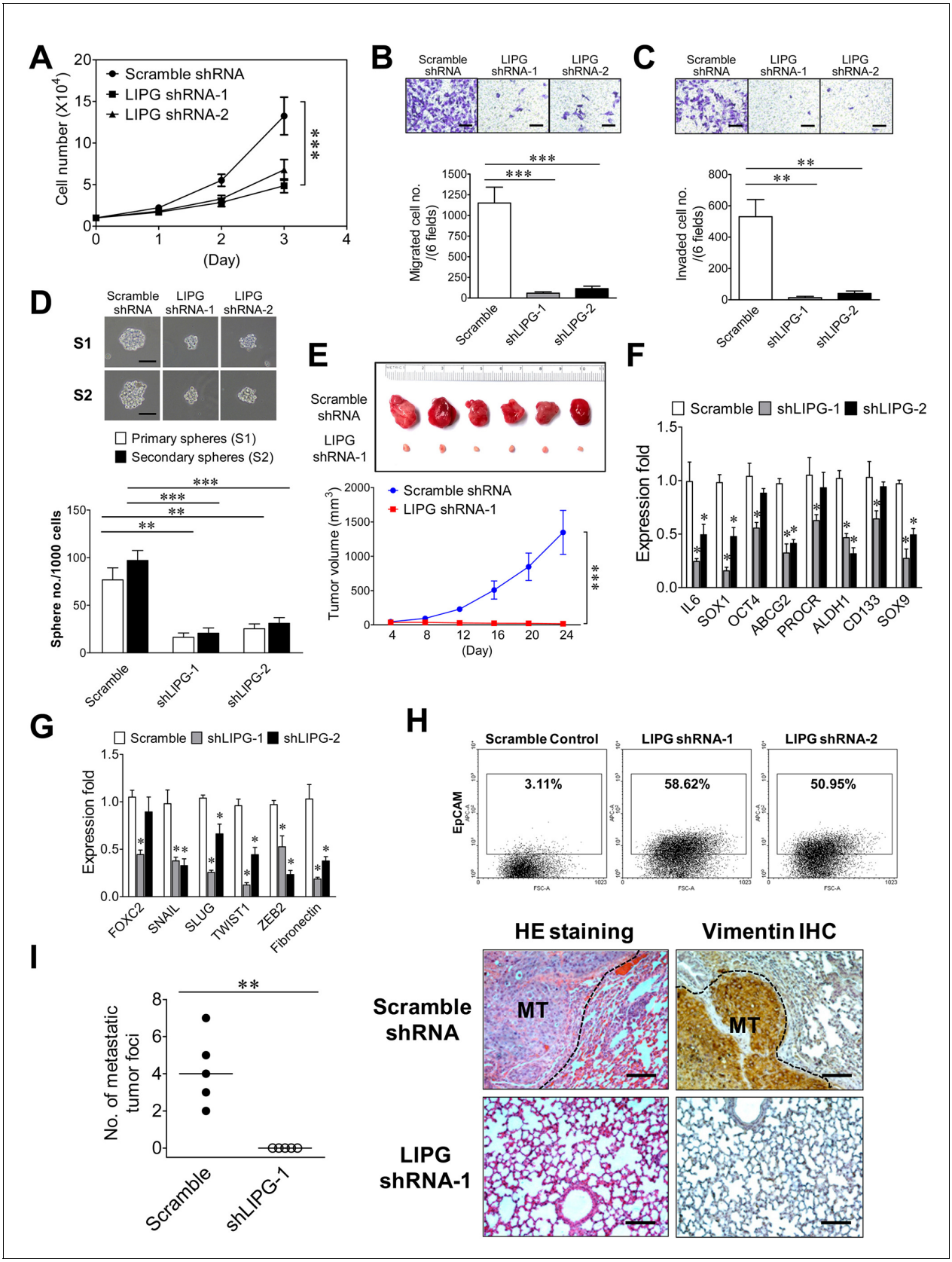

Figure 5. LIPG is required for tumorigenicity and metastasis of basal-like TNBC cells. (**A**) LIPG inactivation attenuates *in vitro* cell growth of MDA-MB-468. 1 × 10^4 cells of shRNA-expressing cells were seeded for the 3-day cell growth study. (**B**) LIPG depletion impairs migration of MDA-MB-468 cells.

Figure 5 continued on next page

Figure 5 continued

The scale bar indicates 100 μm. (**C**) LIPG deficiency inhibits invasion of MDA-MB-468 cells. The scale bar indicates 100 μm. (**D**) LIPG knockdown suppresses primary and secondary CSC sphere formation of MDA-MB-468. The scale bar indicates 50 μm. (**E**) Loss of LIPG abrogates *in vivo* tumor formation of MDA-MB-468. 5×10^6 of scramble or LIPG shRNA-expressing MDA-MB-468 cells were transplanted into the mammary fat pads of nude mice for xenograft tumor formation (n = 6 for each experimental group). The picture of isolated tumors and plotted tumor growth curves are shown on the top and bottom panels, respectively. (**F**) LIPG knockdown downregulates the expression of stem cell genes in MDA-MB-468 cells. (**G**) LIPG knockdown downregulates the expression of EMT programming genes in MDA-MB-468 cells. (**H**) LIPG inactivation substantially increases EpCAM+ cells in MDA-MB-468. (**I**) LIPG inactivation abrogates *in vivo* lung metastasis of MDA-MB-468 cells. Tail vein injection of either scramble shRNA-expressing or LIPG shRNA-expressing MDA-MB-468 cells (1×10^6) was performed on nude mice (n = 5 for each experimental group). After 4 weeks, mice were euthanized and dissected to isolate their lungs for HE staining and IHC analysis of vimentin. In contrast to the negativity of vimentin staining in lung tissue, the strong vimentin staining in tumor tissue areas has confirmed that these formed tumor foci were derived from metastasis of MDA-MB-468, a TNBC line expressing the high levels of vimentin according to the immunofluorescence study. Metastatic tumor foci were counted according to HE and IHC staining results. Representative HE and IHC staining pictures are shown on the right panel and the statistical analysis of metastatic tumor foci is shown on the left panel. The medians (indicated by horizontal lines) for both experimental groups are shown in the plot. The metastatic tumor (MT) tissue areas in the lung HE and IHC staining pictures are indicated by the black dash line. The scale bar indicates 100 μm. Error, SD (n = 3); *p<0.05; **p<0.01; ***p<0.001.

DOI: https://doi.org/10.7554/eLife.31334.019

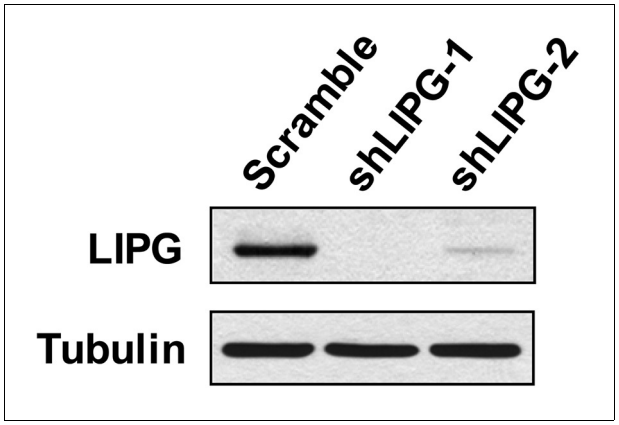

Figure 5—figure supplement 1. Western blot analysis of LIPG and tubulin protein expression in MDA-MB-468 cells with or without LIPG knockdown by two different shRNAs.
DOI: https://doi.org/10.7554/eLife.31334.020

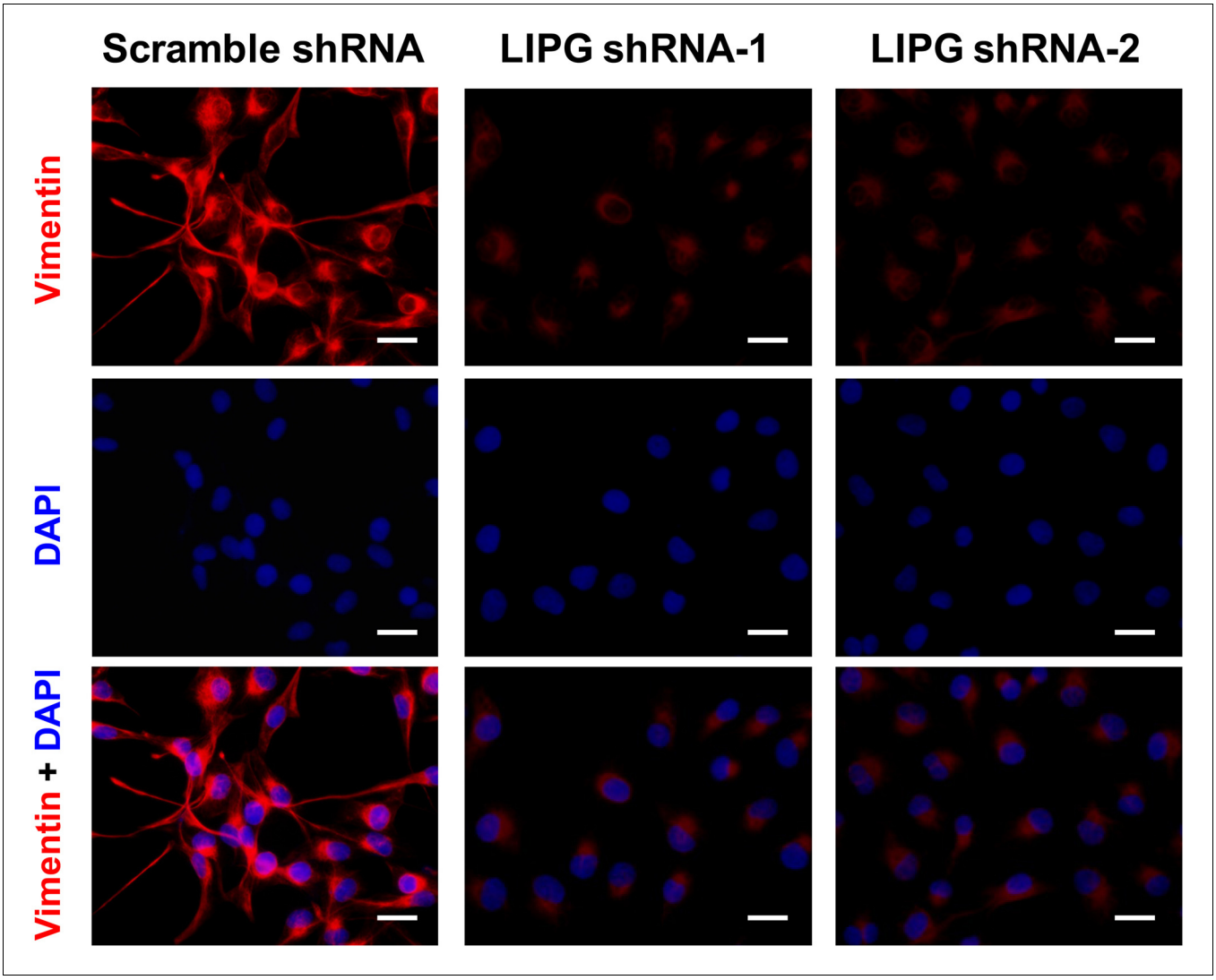

Figure 5—figure supplement 2. Immunofluorescent analysis of vimentin protein expression was performed on MDA-MB-468 lines expressing either the scramble shRNA or two different LIPG shRNAs. Cellular DNA was stained with DAPI. The scale bar indicates 25 μm.

DOI: https://doi.org/10.7554/eLife.31334.021

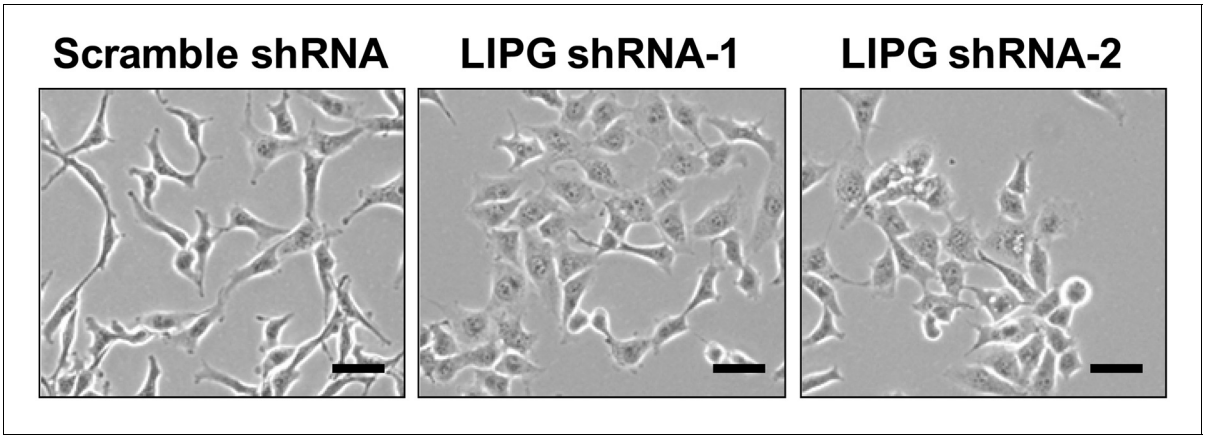

Figure 5—figure supplement 3. LIPG knockdown by two different shRNAs induced a morphological change in MDA-MB-468 cells from a mesenchymal-like phenotype to an epithelial-like phenotype. The scale bar indicates 50 μm.
DOI: https://doi.org/10.7554/eLife.31334.022

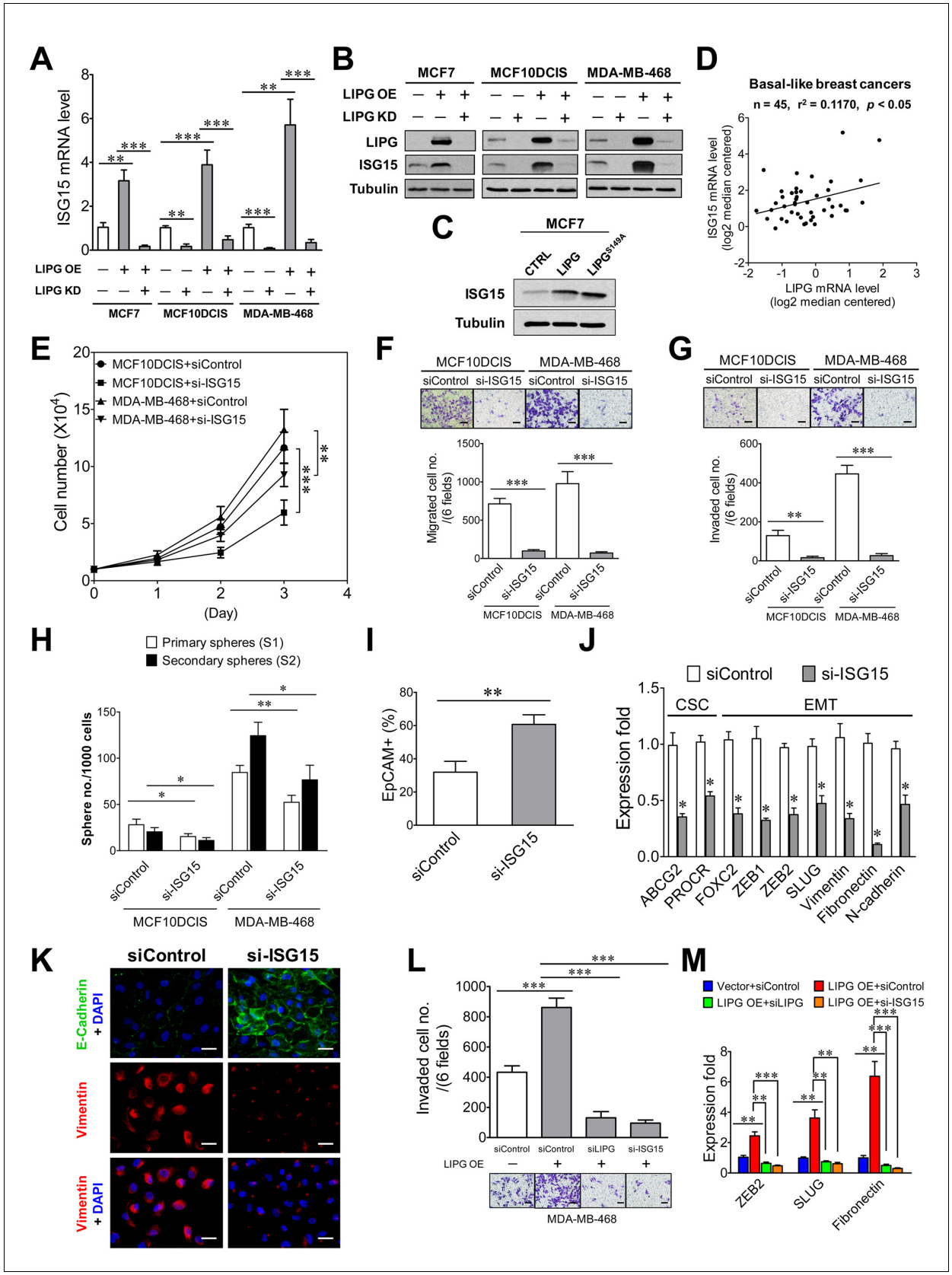

Figure 6. ISG15 is the downstream mediator of oncogenic LIPG signaling in basal-like TNBC cells. (**A**) ISG15 mRNA expression is LIPG-dependent. qRT-PCR analysis of ISG15 mRNA expression was performed on indicated cells with or without LIPG overexpression (LIPG OE) in combination with or

Figure 6 continued on next page

Figure 6 continued

without LIPG knockdown (LIPG KD). (**B**) ISG15 protein expression is LIPG-dependent. Western blot analysis of LIPG, ISG15 and tubulin was performed on protein lysates isolated from cell samples as described in (**A**). (**C**) The lipase catalytic activity of LIPG is dispensable for LIPG-dependent expression of ISG15. Western blot analysis of ISG15 and tubulin was performed on vector-control, wild-type LIPG-overexpressing and $LIPG^{S149A}$-overexpressing MCF7 cells. (**D**) ISG15 mRNA expression is positively correlated with LIPG expression in human basal-like breast cancers. The linear regression correlation was plotted based on *in silico* analysis of ISG15 and LIPG mRNA levels in 45 cases of BLBC derived from the Gluck dataset collected in the Oncomine database. (**E**) ISG15 knockdown impairs cell growth of MCF10DCIS and MDA-MB-468. (**F**) ISG15 knockdown inhibits migration of MCF10DCIS and MDA-MB-468 cells. The scale bar indicates 100 μm. (**G**) ISG15 knockdown suppresses invasion of MCF10DCIS and MDA-MB-468. The scale bar indicates 100 μm. (**H**) ISG15 knockdown attenuates primary and secondary CSC sphere formation of MCF10DCIS and MDA-MB-468. (**I**) ISG15 knockdown increases EpCAM+ cells in MCF10DCIS. (**J**) ISG15 knockdown downregulates the expression of stem cell and EMT genes in MCF10DCIS cells. (**K**) ISG15 knockdown leads to E-cadherin upregulation and vimentin downregulation in MCF10DCIS cells. The scale bar indicates 25 μm. (**L**) ISG15 is required for LIPG overexpression-promoted invasion of MDA-MB-468. Transwell-based invasion analysis was performed on parental control MDA-MB-468 cells and LIPG-overexpressing cells with or without knockdown of either LIPG or ISG15. The scale bar indicates 100 μm. (**M**) ISG15 is required for LIPG-overexpression-enhanced expression of EMT genes in MDA-MB-468 cells. qRT-PCR analysis of three EMT genes was performed on mRNA samples isolated from cells as described in (**L**). Error, SD (n = 3); *p<0.05; **p<0.01; ***p<0.001.

DOI: https://doi.org/10.7554/eLife.31334.024

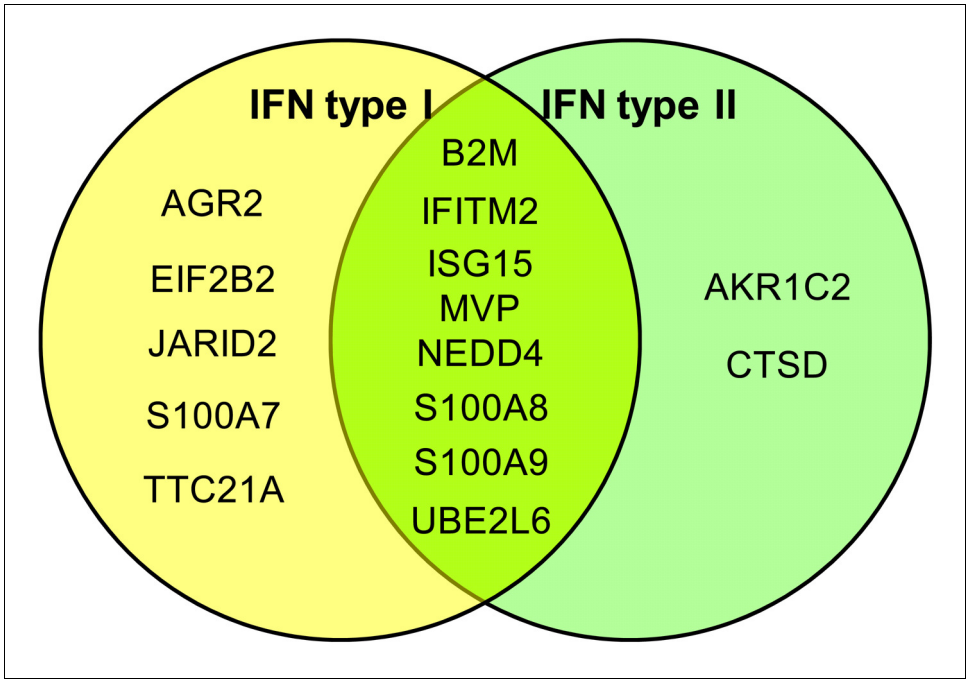

Figure 6—figure supplement 1. LIPG overexpression in luminal MCF7 breast cancer cells leads to increased expression of interferon-stimulated genes (ISGs). Proteomic profiling analysis was performed on MCF7-CTRL and MCF7-LIPG cells. The expression folds of identified proteins are the relative folds of MCF7-LIPG vs. MCF7-CTRL. Among upregulated proteins (the fold ≥2.0) we identified in MCF7-LIPG cells, 15 proteins belong to interferon-stimulated genes (ISGs). ISGs of IFN type I and II are shown in the Venn diagram. Interferome, a curated online database of ISGs (www.interferome.org), was used to classify the IFN type of these ISGs identified from the proteomic studies.

DOI: https://doi.org/10.7554/eLife.31334.025

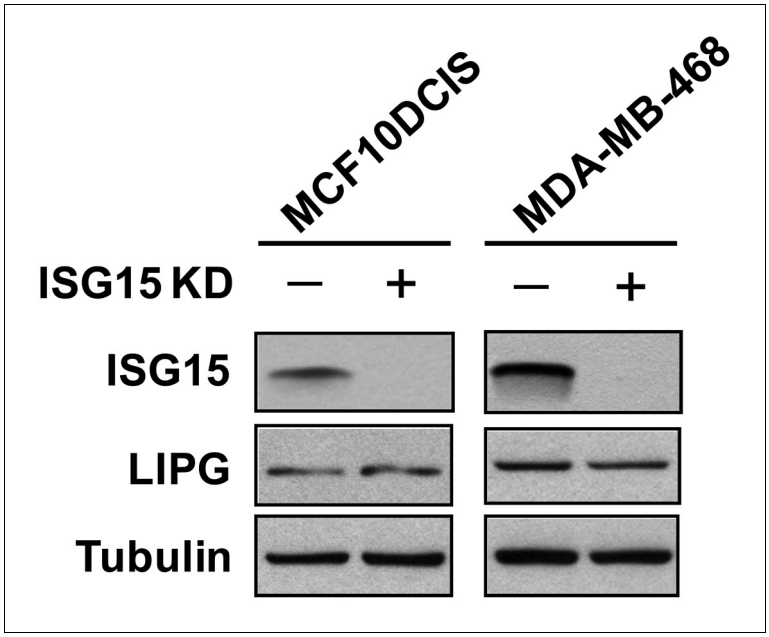

Figure 6—figure supplement 2. Western blot analysis of ISG15, LIPG and tubulin protein expression in MCF10DCIS and MDA-MB468 cells with or without ISG15 knockdown.

DOI: https://doi.org/10.7554/eLife.31334.026

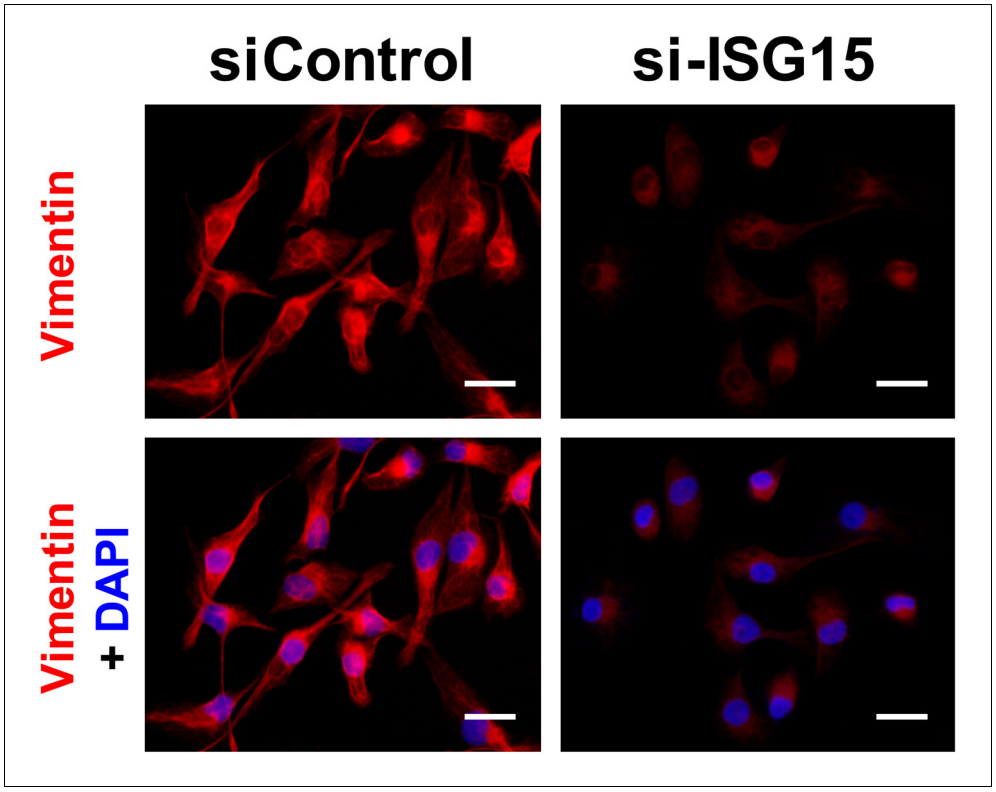

Figure 6—figure supplement 3. Immunofluorescent analysis of vimentin protein expression was performed on either control siRNA-(siControl)-transfected or ISG15 siRNA (si-ISG15)-transfected MDA-MB-468 cells. Cellular DNA was stained with DAPI. The scale bar indicates 25 μm.

DOI: https://doi.org/10.7554/eLife.31334.027

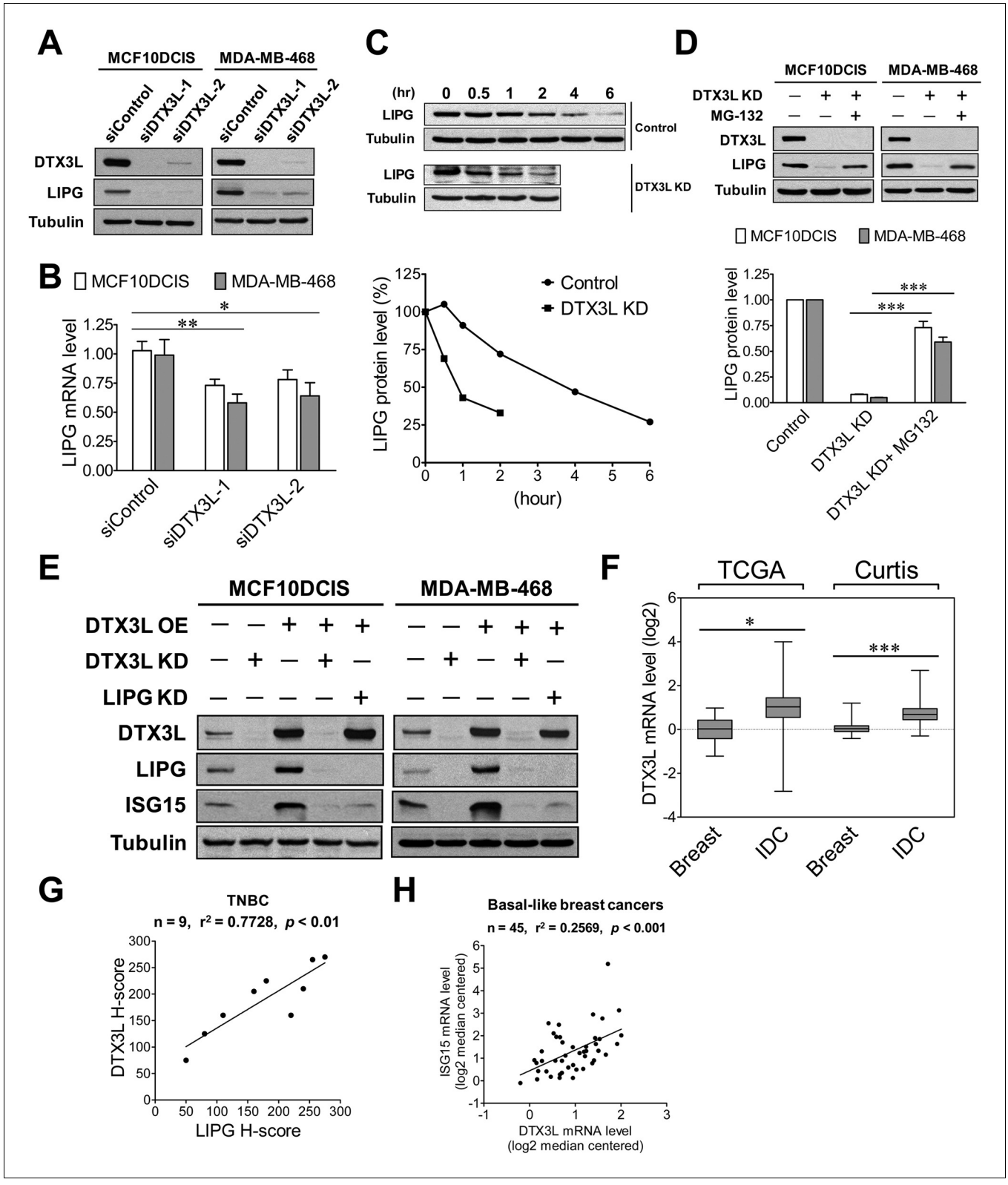

Figure 7. DTX3L is the upstream activator of the LIPG-ISG15 signaling axis in basal-like TNBC cells. (**A**) DTX3L inactivation leads to a dramatic reduction in LIPG protein expression in MCF10DCIS and MDA-MB-468. Western blot analysis of DTX3L, LIPG and tubulin was performed on MCF10DCIS and MDA-MB-468 cells with or without DTX3L knockdown by two different siRNAs. (**B**) DTX3L knockdown results in a modest decrease in LIPG mRNA levels in MCF10DCIS and MDA-MB-468 cells. qRT-PCR analysis of LIPG mRNA expression was performed on siRNA-transfected cells as

Figure 7 continued on next page

Figure 7 continued

described in (**A**). (**C**) DTX3L deficiency shortens the half-life of LIPG protein in MDA-MB-468 cells. After treatment with the protein synthesis inhibitor cycloheximide (200 μg/ml), MDA-MB-468 cells with or without DTX3L knockdown were harvested at different time points as indicated for western blot analysis of LIPG and tubulin. Kinetic changes in LIPG protein levels during the time course are shown in the quantitative plot on the bottom panel. (**D**) DTX3L depletion facilitates proteasome-mediated LIPG protein degradation. Western blot analysis of DTX3L, LIPG and tubulin was performed on control and DTX3L-knockdown MDA-MB-468 cells with or without MG-132 treatment (10 μM) for 10 hr. The quantitative data are shown on the bottom panel. (**E**) The DTX3L-LIPG signaling axis is required for ISG15 expression in MCF10DCIS and MDA-MB-468 cells. Western blot analysis of DTX3L, LIPG, ISG15 and tubulin was performed on MCF10DCIS and MDA-MB-468 cells with or without DTX3L knockdown, and on their respective DTX3L-overexpressing cells with or without knockdown of either DTX3L or LIPG. (**F**) DTX3L is aberrantly overexpressed in breast cancer. DTX3L mRNA expression in normal breast and IDC was analyzed *in silico* using the TCGA and Curtis datasets. TCGA: breast (n = 61), IDC (n = 389); Curtis: breast (n = 144), IDC (n = 1556). The 25th and 75th percentiles are indicated as a vertical box and the minimal and maximal data values are indicated as outliers. (**G**) DTX3L protein expression positively correlates with LIPG expression in TNBC. IHC analysis of DTX3L and LIPG was performed on nine cases of TNBC. The linear regression correlation was plotted based on H-scores of DTX3L and LIPG IHC-stained TNBC cases. (**H**) DTX3L mRNA expression is positively associated with ISG15 expression in human basal-like breast cancers. The linear regression correlation was plotted based on *in silico* analysis of DTX3L and ISG15 expression in 45 cases of BLBCs derived from the Gluck dataset. Error, SD (n = 3); *p<0.05; **p<0.01; ***p<0.001.
DOI: https://doi.org/10.7554/eLife.31334.030

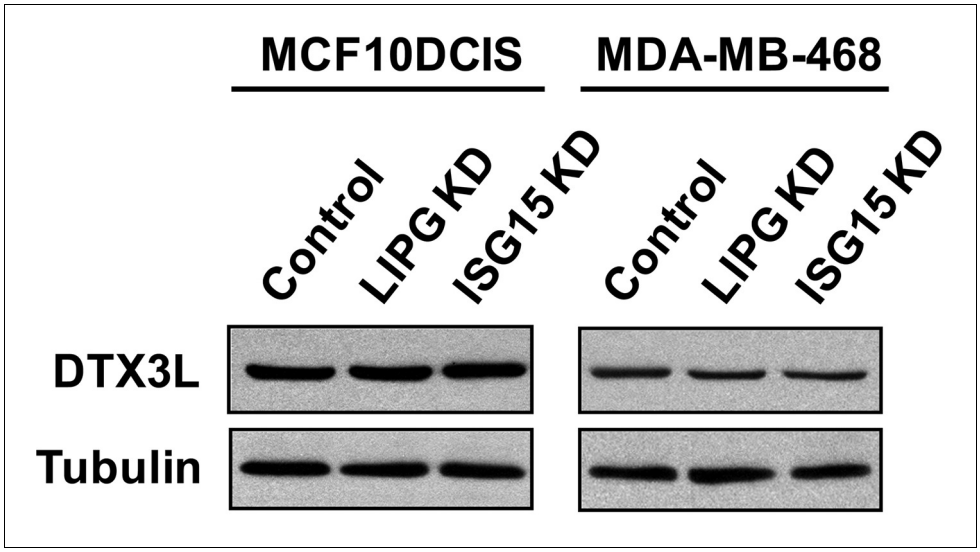

Figure 7—figure supplement 1. Western blot analysis of DTX3L and tubulin protein expression in MCF10DCIS and MDA-MB-468 cells with or without knockdown of either LIPG or ISG15.
DOI: https://doi.org/10.7554/eLife.31334.031

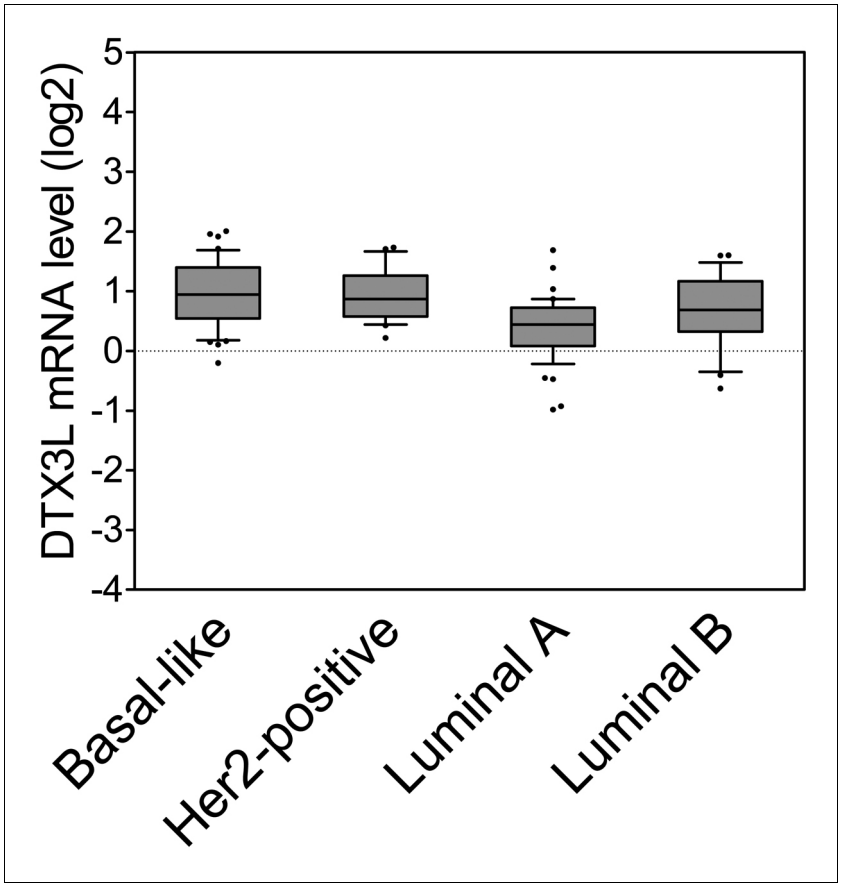

Figure 7—figure supplement 2. Expression of DTX3L mRNA in basal-like (n = 45), HER2+ (n = 21), luminal-A (n = 46) and luminal-B (n = 25) subtypes of breast cancer.
DOI: https://doi.org/10.7554/eLife.31334.032

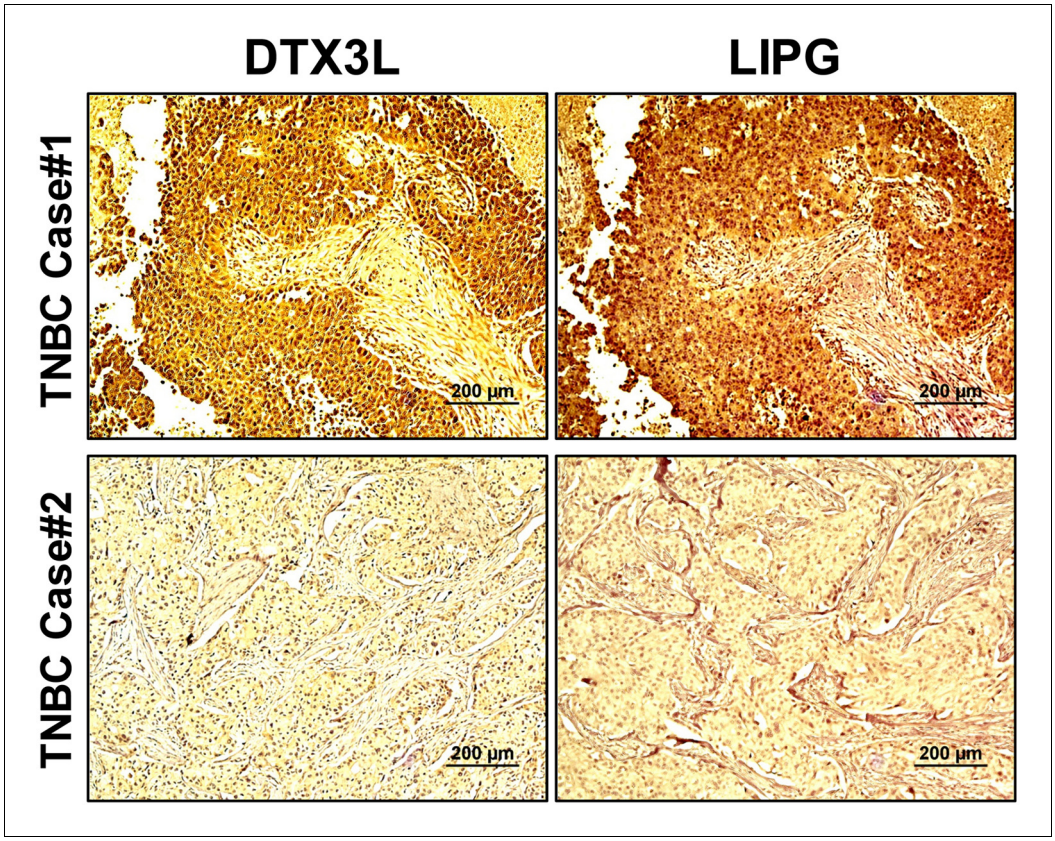

Figure 7—figure supplement 3. LIPG protein expression is positively associated with DTX3L protein expression in TNBCs. IHC analysis of DTX3L and LIPG protein expression was performed on TNBC tissues. DTX3L and LIPG were concurrently expressed at high and low levels in TNBC case#1 and case#2, respectively.
DOI: https://doi.org/10.7554/eLife.31334.033

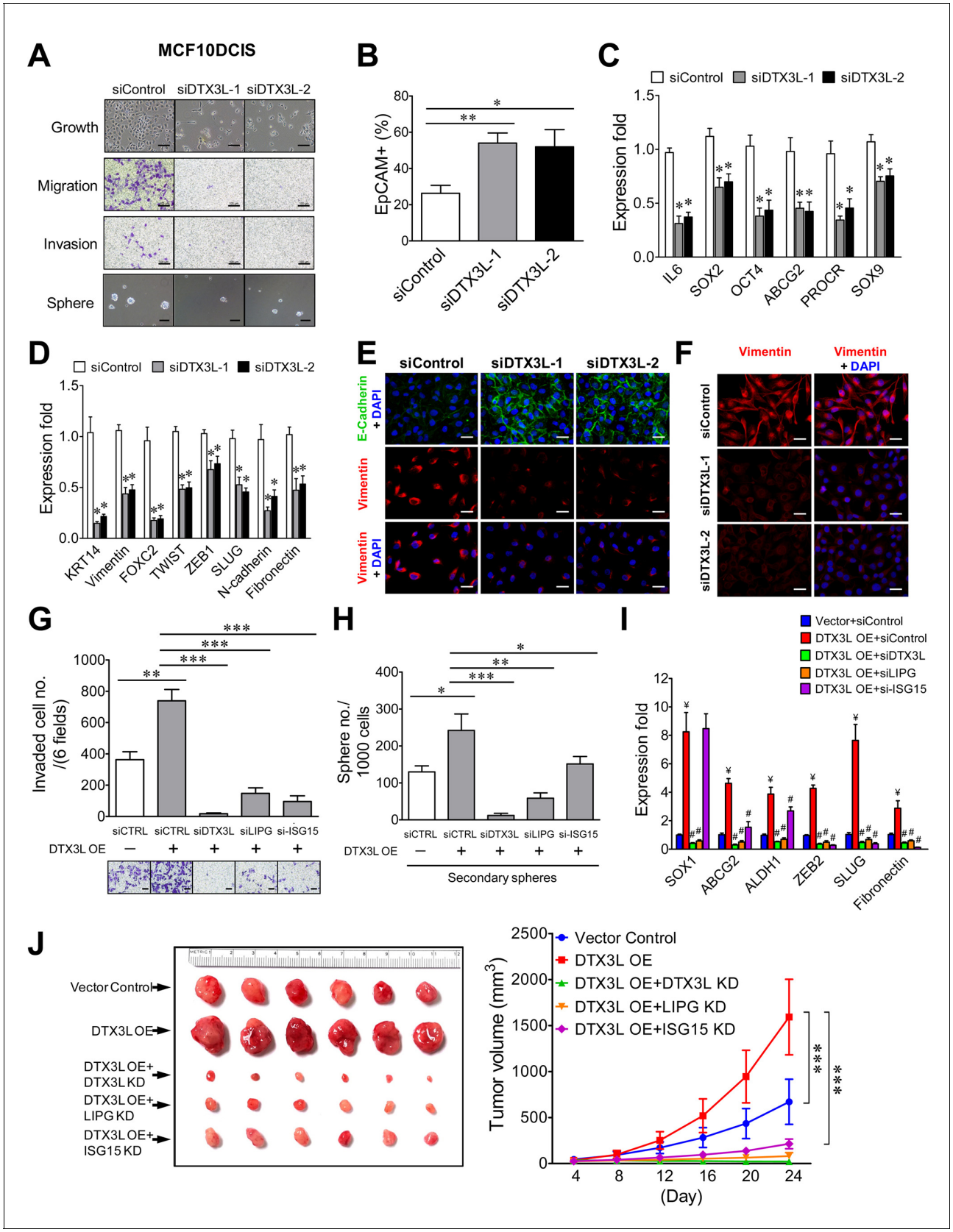

Figure 8. The DTX3L-LIPG-ISG15 signaling axis is essential for malignancies of LIPG-expressing TNBC cells *in vitro* and *in vivo*. (**A**) DTX3L knockdown inhibits growth, migration, invasion and CSC sphere formation of MCF10DCIS cells. The scale bars indicate 100 μm. (**B**) DTX3L knockdown increases

Figure 8 continued on next page

Figure 8 continued

EpCAM+ cells in MCF10DCIS. (**C**) DTX3L inactivation downregulates the expression of multiple stem cell genes in MCF10DCIS cells. (**D**) DTX3L depletion induces the decreased expression of multiple basal/EMT genes in MCF10DCIS cells. (**E**) DTX3L knockdown leads to E-cadherin upregulation and vimentin downregulation in MCF10DCIS cells. The scale bar indicates 25 μm. (**F**) DTX3L knockdown results in vimentin downregulation in MDA-MB-468 cells. The scale bar indicates 25 μm. (**G**) The LIPG-ISG15 axis mediates DTX3L overexpression-enhanced invasion of MDA-MB-468 cells. Transwell-based invasion analysis was performed on DTX3L-overexpressing MDA-MB-468 cells with or without siRNA-mediated knockdown of a gene component in the DTX3L-LIPG-ISG15 axis and parental control cells. (**H**) The LIPG-ISG15 axis mediates DTX3L overexpression-promoted secondary CSC sphere formation of MDA-MB-468 cells. Secondary CSC sphere formation analysis was performed on cells as described in (**G**). (**I**) The LIPG-ISG15 axis mediates DTX3L overexpression-induced increases in expression of stem cell and EMT genes in MDA-MB-468 cells. qRT-PCR analysis of three stem cell and three EMT genes was performed on cells as describe in (**G**). ¥ $p<0.01$ versus the control dataset (Vector + siControl); # $p<0.05$ versus the dataset of MDA-MB-468-DTX3L OE cells transfected with siControl (DTX3L OE +siControl). (**J**) The DTX3L-LIPG-ISG15 axis is required for *in vivo* tumor formation of MDA-MB-468 cells in nude mice. 1×10^6 of DTX3L-overexpressing MDA-MB-468 cells with or without shRNA-mediated knockdown of a gene component in the DTX3L-LIPG-ISG15 axis or parental control cells were transplanted into the mammary fat pads of nude mice for xenograft tumor formation. The picture of isolated tumors and plotted tumor growth curves are shown on the left and right panels, respectively. Error, SD (n = 3); *$p<0.05$; **$p<0.01$; ***$p<0.001$.

DOI: https://doi.org/10.7554/eLife.31334.038